

Far-infrared optical properties of the pyrochlore spin ice compound $\text{Dy}_2\text{Ti}_2\text{O}_7$

C.Z. Bi^{†‡} J.Y. Ma[†] B.R. Zhao[†] Z. Tang[‡] D. Yin[‡] C.Z. Li[‡]
D.Z. Yao[‡] J. Shi[‡] and X.G. Qiu^{† ‡}

[†] National Laboratory for Superconductivity, Institute of Physics,
Chinese Academy of Sciences, P.O. Box 603, Beijing 100080, China

[‡] Department of Physics, Wuhan University, Wuhan, Hubei 430072, China

Abstract. Near normal incident far-infrared reflectivity spectra of [111] dysprosium titanate ($\text{Dy}_2\text{Ti}_2\text{O}_7$) single crystal have been measured at different temperatures. Seven phonon modes (eight at low temperature) are identified at frequency below 1000 cm^{-1} . Optical conductivity spectra are obtained by fitting all the reflectivity spectra with the factorized form of the dielectric function. Both the Born effective charges and the static optical permittivity are found to increase with decreasing temperature. Moreover, phonon linewidth narrowing and phonon modes shift with decreasing temperature are also observed, which may result from enhanced charge localization. The redshift of several low frequency modes is attributed to the spin-phonon coupling. All observed optical properties can be explained within the framework of nearest neighbor ferromagnetic(FM) spin ice model.

PACS numbers: 78.30.-j, 78.20.-e, 63.20.-e, 77.22.ch

1. Introduction

Recently, there has been a surge of interest in the properties of pyrochlore compound $Dy_2Ti_2O_7$, which is considered to be a model system of “spin ice” materials. “Spin ice” materials governed by the same statistical mechanics of so-called “ice rule” as the hydrogen atoms in the ground state of ordinary hexagonal ice I_h have macroscopically degenerate ground states down to almost zero temperature.[1, 2, 3, 4, 5, 6, 7, 8, 9] Experimentally, the observed value of $(1/2)R\ln(3/2)$ through specific heat measurement[1] is consistent with what is expected by Pauling’s theory, while the spin entropy only freezes out below about 4 K.[2] From magnetic susceptibility studies, a strongly frequency dependent cooperative spin freezing is observed at about 16 K, which is associated with a very narrow distribution of spin relaxation times and a sharp drop at about 2 K.[3, 6] Neutron scattering studies performed by Fennell et al.[4] also well demonstrate the spin ice state and the coexistence of long range ferromagnetic and short range antiferromagnetic order in a magnetic field applied along the [110] axis of $Dy_2Ti_2O_7$. In theoretical aspect, R.G. Melko and coworkers[7] report numerical results on the low temperature properties of the dipolar spin ice model by the multicanonical Monte Carlo (MC) method and they find a first order transition to a long-range ordered phase. Other researchers[8] also confirm the existence of the transition under a magnetic field along the [110] axis with MC simulation.

$Dy_2Ti_2O_7$ has a typical $A_2B_2O_7$ structure with the space group (Fd3m, O_h^7), No.227. B cation is sixfold coordinated and locates at the center of the distorted octahedron formed by corner O ions. The A-site ions, i.e., Dy^{3+} (a magnetic rare-earth ion with effective spin $S=1/2$) resides on a lattice of corner-sharing tetrahedral, as shown in figure 1 of reference 3. In the Dy^{3+} sublattice topology the spin configuration with two spins pointing directly towards while two spins pointing directly away from the center of the tetrahedral corresponds to the analogous proton disorder in real ice. Then a ferromagnetic and dipolar nearest-neighbor spin-spin interaction leads to a strong geometrical frustration, preventing the system from long range ordering. As a result, high degeneracy of spin states will occur at low temperature.

Owing to the Ising anisotropy arising from crystal-field effect in the pyrochlore lattice, the macroscopically degenerate states when the field is along the [111] direction are different from those for other field directions. For the [111] direction, the frustration structure changes from that of a three-dimensional pyrochlore to that of a two-dimensional Kagome-like lattice with constraint, leading to different values of the zero-point entropy.[5] The combination of ferromagnetic coupling and Ising anisotropy may be a reason for the strong frustration. But how the spins interact with each other is not well understood in the spin ice materials.

Up to now, there has been no experimental report on the infrared optical properties of $Dy_2Ti_2O_7$. IR spectroscopy can give insight to the dynamical processes related to phonon, charge carrier, and spin. Motivated by this situation, we studied the infrared reflectivity of $Dy_2Ti_2O_7$ single crystal on the [111] plane from room temperature down

to 10 K. The temperature dependence of phonon modes is obtained, and the role played by spin-phonon coupling on the phonon modes is being discussed.

2. Experimental details

Dy₂Ti₂O₇ single crystal was prepared by the floating zone method, using an infrared furnace equipped with two elliptical mirrors. Before the single crystal growth, the polycrystalline rods was prepared by a standard solid state reaction. Stoichiometric mixture of Dy₂O₃ (CERAC, 99.99%) and TiO₂ (CERAC, 99.9%) was heated in air at 1250°C for five days with intermediate regrinding to ensure complete reaction. The typical growth condition was 4.5 mm/h for both feed and growth speeds. To avoid oxygen deficiency, the single crystal was grown in an O₂ atmosphere of 0.3 MPa. The single crystal obtained was translucent yellow. Powder x-ray diffraction measurements on the crystal confirmed that the product was a single phase with cubic pyrochlore structure and the parameter of the unit cell was a=10.1122Å. The principal axes were determined using Laue diffraction pattern.

The crystal was cleaved and one-side polished with the surface parallel to the [111] plane. The reflectivity spectra R(ω) at different temperatures were measured at near-normal incidence of about 8° on a Bomen DA8 Fourier transform infrared spectrometer, in the range from 50 to 6500 cm⁻¹. In the far infrared region, a He cooled bolometer and 6 mm mylar beamsplitter were used. In the middle infrared region, a liquid nitrogen cooled mercury cadmium telluride detector and KBr beamsplitter were utilized. To obtain the absolute reflectivity, an evaporated golden mirror was served as a reference. Spectra were collected with a resolution of 4 cm⁻¹. The samples were mounted in a continuous helium flow cryostat in which the temperature could be varied between 300 and 10 K.

3. Results and discussion

The temperature dependent reflectivity of the Dy₂Ti₂O₇ single crystal shown in figure 1 is typical that of a nonmetallic system. The sharp features in the reflectivity spectra are due to the unscreened infrared active optical phonon modes, above the highest observed lattice vibration frequency, the reflectivity is flat and featureless up to the highest measured frequency. It can be seen that the reflectivity within the reststrahlen bands increases with decreasing temperature. At high temperature seven modes can easily be identified.

The mode frequencies are obtained from a damped harmonic oscillator fit of reflectivity spectra with a complex dielectric function ε(ω) in the factorized form (generalized Lyddane-Sachs-Teller relation) [10, 11]:

$$\varepsilon(\omega) = \varepsilon_1(\omega) + \varepsilon_2(\omega) = \varepsilon_\infty \prod_{j=1}^n \frac{\Omega_{jLO}^2 - \omega^2 - i\gamma_{jLO}\omega}{\Omega_{jTO}^2 - \omega^2 - i\gamma_{jTO}\omega}, \quad (1)$$

where ε_∞ represents the high frequency dielectric constant (at frequencies large compared with the lattice vibration frequencies but small compared with the electronic transition frequencies), Ω_{jLO} and Ω_{jTO} are the longitudinal and transverse eigenfrequencies of the j th optical phonon mode, γ_{jLO} and γ_{jTO} represent their longitudinal and transverse damping constants. Using this dielectric function, all the reflectivity spectra in our measurements were fitted with the well known Fresnel formula for reflectivity of a half space medium in vacuum[12]:

$$R(\omega) = \left| \frac{\sqrt{\varepsilon(\omega)} - 1}{\sqrt{\varepsilon(\omega)} + 1} \right|^2 \quad (2)$$

Based on equation (1) and (2), a fit of $R(\omega)$ to the observed reflectivity spectra can be obtained with a proper choice of the model parameters Ω_{jLO} , Ω_{jTO} , γ_{jLO} , γ_{jTO} and ε_∞ . Adjustment of the parameters is made by trial and error fitting of formula (2) to the experimental spectra. This method yields not only $\varepsilon(\omega)$ but also the model parameters which characterize the infrared active phonons.

From a group theoretical analysis,[13] a compound with the pyrochlore structure symmetry should have the vibrational phonon modes at the Brillouin zone center Γ point with

$$\Gamma = 8 F_{1u} + 4 F_{2u} + 2 F_{1g} + 4 F_{2g} + 3 E_u + E_g + A_{1g} + 3 A_{2u}.$$

Among these 26 normal modes, only A_{1g} , E_g , $4 F_{2g}$ are Raman active, $7 F_{1u}$ are infrared active, and one F_{1u} acoustical. Consequently, the observed phonons in the spectra of Dy₂Ti₂O₇ at low temperature except that at about 610 cm⁻¹ were denoted sequentially from low to high frequencies by F_{1u}^1 to F_{1u}^7 . The number is in good agreement with the group theoretical analysis. The mode at 610 cm⁻¹, denoted by F_{1u}^{7*} , is weak in intensity and does not change with the temperature. It is probably originated from two phonon absorption because of its low intensity.[14]

The fitting results of the oscillator parameters for all the phonon modes of Dy₂Ti₂O₇ are summarized in Table 1. The high frequency dielectric constant is adopted as 5.0. Figure 2 shows the experimental and fitting curves at two representative temperatures of 300 K and 10 K. The fitting results with the Lorentz oscillators could explain the global features of the phonon spectra reasonably well, even though some difference between the experimental and the fitted data remains. A small deviation of the calculated curves from the experimental one is seen on the low frequency edge of F_{1u}^2 mode in the high temperature. A possible reason is the reflection from the rear surface of the sample due to its transparency at low frequencies as well as the cutoff of the working frequency of the detector. However, the deviation has few impact on other phonon fitting parameters in other frequency range.

The real part of the optical conductivity $\sigma_1(\omega)$ can be extracted from $\varepsilon_2(\omega)$, where $\sigma_1(\omega) = 1.6638 \cdot 10^{-2} \omega \varepsilon_2(\omega)$, here ω is in unit of cm⁻¹ and σ_1 in unit of $\Omega^{-1} \text{ cm}^{-1}$, the corresponding result is shown in figure 3.[15] The conductivity is dominated by seven peak structures due to optical phonon absorption, no free carrier contribution can be observed. For normal materials, with decreasing T, the anharmonic thermal

motion would decrease, which results in a decrease in the lattice constant. Then the phonons should shift to higher frequencies and their linewidth should become narrower. The F_{1u}⁶ mode has clearly demonstrated this effect. Its center frequency shifts from 439 cm⁻¹ to 452 cm⁻¹ as the temperature decreases from 300 K down to 10 K. Moreover, the phonon peak is more and more prominent and separated from the nearby mode F_{1u}⁵. But it is puzzling that other modes do not exhibit the same behavior, the three most prominent phonons, F_{1u}², F_{1u}³ and F_{1u}⁵, show discernible redshifts. Coupling of phonons to magnetic excitations in solids may result in a change of phonon self-energy, i.e., the frequency due to spin-phonon interaction. Therefore, spin-phonon coupling[16] closely correlated with the Dy³⁺ (its effective spin S=1/2) could be a possible origin for the abnormal temperature dependence of the phonon frequency. As we mentioned in the introduction, Dy³⁺ cations can have appreciable magnetic moments. Consequently, ferromagnetic nearest neighbor dipole-dipole interactions will present in spin ice Dy₂Ti₂O₇ in which large dipole interactions have been suggested to be responsible for the spin ice behavior.[17] These effects have been quantitatively confirmed by both experimental and theoretical approaches.[9] At the nearest neighboring sites, the exchange interactions between the magnetic atoms become the strongest. Subsequently, the crystal potential U can be described as following:

$$U = \frac{1}{2}kx^2 + \sum_{ij} J_{ij} \langle S_i S_j \rangle, \quad (3)$$

where x is the atomic displacement from the equilibrium position in the oscillator model. In the second term, J_{ij} is the exchange energy constant which is a function of the structural parameters, such as the bond lengths between Dy³⁺cations and the corresponding bond angles mediated by the O ions. S_i represents the spin of Dy³⁺cation at the ith site. < S_iS_j > denotes a statistical average over the adjacent spins. The harmonic force constant derived from its second derivative formula reads:

$$\frac{\partial^2 U}{\partial x^2} = k + \sum_{ij} \left(\frac{\partial^2 J_{ij}}{\partial x^2} \right) \langle S_i S_j \rangle. \quad (4)$$

Note that the second term represents the spin-phonon coupling, which suggests that the phonon frequency should have an additional contribution. As for the spin-phonon coupling coefficient, $\sum_{ij} \left(\frac{\partial^2 J_{ij}}{\partial x^2} \right)$ can be different for each phonon and can have either a positive or a negative sign. Furthermore, different phonon frequencies will have redshift or blueshift in the optical conductivity spectra. As the temperature decreases, spin fluctuation becomes weaker and spin-phonon coupling stronger. It is important to notice that although ferromagnetic correlations are short ranged without long range order in spin ice compounds, from neutron scattering measurements Harris et al.[18] have shown that the range of ferromagnetic order increases at lower temperature. As a result, spin-phonon coupling range is wider so that the phonon frequency shows redshift or blueshift, which is in agreement with what is observed in our optical conductivity spectra.

Now we focus on the remarkable change of the spectra weight which is proportional to the area under the optical conductivity peak. It is well known that, by decreasing the temperature, thermal fluctuation reduces, which may result in narrowing in the linewidth and enhancement in the oscillator strength without any changes in the bonding or coordination. Almost all phonon modes exhibit the theoretically predicted behavior in our optical conductivity spectra. But the spectral weight should not change. The anomalous increase in oscillator strength of the low-frequency modes must be taken sufficient care of. Optical sum rules provide a powerful tool with which to analyze the behavior of free carriers and bound excitations.[19] The partial conductivity sum rules corresponding primarily to a single class of absorption such as excitation of phonons, conduction, valence, or core electrons have been developed. For oscillator states, the partial conductivity sum rule can be expressed as [20]

$$\frac{120}{\pi} \int_{\omega_a}^{\omega_b} \sigma_1(\omega) d\omega = \omega_{p,j}^2, \quad (5)$$

where ω_a , ω_b and $\omega_{p,j}$ (in unit of cm^{-1}) are the integral lower and upper limits and effective plasma frequency associated with the isolated phonon absorption, respectively. In the above equation, σ is in unit of $\Omega^{-1} \text{cm}^{-1}$. The integral region of the j th oscillator should be chosen to cover the full spectral weight. The dramatic increase in the spectra weight has implications for the distribution of charge and the change in local strength of the binding charge. The effective charge of Dy, Ti and O ions in the unit cell with k atoms can be determined through the following Equation (6)(in Gauss unit system)[21]

$$\frac{1}{\varepsilon_\infty} \sum_j \omega_{p,j}^2 = \frac{4\pi}{V_c} \sum_k \frac{(Z_k^* e)^2}{M_k}, \quad (6)$$

where V_c is the unit cell volume, j and k index the lattice modes and the atoms with mass M_k , respectively. For the effective charge, there is a general expression $\sum_k Z_k^* = 0$.

In $Dy_2Ti_2O_7$, oxygen is the lightest element, therefore, in the right side of equation (6), the summation is dominated by O ion item and the terms for Dy ion and Ti ion may be neglected. The change in the effective charge is associated mainly with the oxygen (i.e., $Z_k^* \approx Z_o^*$). Combining equation (5) and equation (6), we obtain the value for Z_o^* as shown in figure 4. The absolute value of Z_o^* is of less significance, what is important is the temperature dependence of the deduced value for Z_o^* , which increases with decreasing temperature. When the incident light couples to the induced dipole moments created by the atomic displacements associated with a normal mode, if the Born effective charge per oxygen atom Z_o^* is increasing, then the size of the induced dipole moment and the optical absorption will also increase, which well explain the above temperature dependence of the optical conductivity. On the other hand, the increase in Z_o^* means a change in the bond length and bond angle between O ion and cations so that the bond lengths between Dy^{3+} cations and the corresponding bond angles mediated by the O ions will change. Subsequently, J_{ij} and $\langle S_i S_j \rangle$ have different changes associated with phonon central frequency shift as we observed above. In summary, the change in the effective charge arising from electrical charge localization strengthening is the fundamental reason why

the spectra weight increases and phonon frequency shifts. From our experimental results, within the framework of the ferromagnetic spin ice model, we consider that the increase in Z_o^* is closely related with nearest-neighbor ferromagnetic interaction strengthening and/or widening in the correlation range. In this simple physical picture, the increasing FM exchange between Dy^{3+} cations will lead to a decrease of the distance between mediated O ion and Dy^{3+} , which enhance the increase in Z_o^* , in agreement with our experimental observation.

LST relationship also provides an effective examination on static optical permittivities ε_0 in the approximation of zero phonon frequency. When $\omega=0$, the equation evolves into the following form:

$$\frac{\varepsilon_0}{\varepsilon_\infty} = \prod_i \frac{\Omega_{iLO}^2}{\Omega_{iTO}^2}. \quad (7)$$

From Equation (7) ε_0 of $Dy_2Ti_2O_7$ single crystal at different temperatures are also obtained, as shown in the inset of figure 4. It exhibits the same temperature dependence as Z_o^* , which suggests that the temperature dependence of ε_0 can be originated from that of Z_o^* and essentially, charge localization arising from FM exchange plays an important role in the temperature variation of both ε_0 and Z_o^* .

4. Conclusions

In conclusion, FIR response of $Dy_2Ti_2O_7$ single crystals has been studied under different temperatures. Seven infrared active phonons have been observed, which agrees well with a group analysis. All the spectra are fitted with the oscillator model and an excellent agreement between experimental and calculated spectra is obtained. Of all phonons, one shows discernible blueshift and three obvious redshifts with decreasing temperature. The shifts are attributed to the spin-phonon coupling in a geometrically frustrated configuration in the spin ice material. The oscillation strength of the low frequency modes increase dramatically at low temperature, indicating that the Born effective charges are increasing in the unit cell. We propose that the similar temperature dependence of the static optical permittivity with Born effective charge may originate from the intrinsic charge localization resulted from the nearest-neighbor FM interaction.

Acknowledgments

This work is supported by National Science Foundation of China (Grants No. 10474128 and No. 10474074).

References

- [1] Ramirez A P, Hayashi A, Cava R J, Siddharthan R and Shastry B S 1999 *Nature (London)* **399** 333
- [2] Snyder J, Ueland B G, Slusky J S, Karunadasa H, Cava R J and Schiffer P 2004 *Phys. Rev. B* **69** 064414

- [3] Snyder J, Slusky J S, Cava R J and Schiffer P 2001 *Nature (London)* **413** 48
- [4] Fennell T, Petrenko O A, Balakrishnan G, Bramwell S T, Champion J D M, Fak B, Harris M J and Paul D M 2002 *Appl. Phys. A* **74** S889
- [5] Higashinaka R, Fukazawa H and Maeno Y 2003 *Phys. Rev. B* **68** 014415
- [6] Matsuhira K, Hinatsu Y and Sakakibara T 2001 *J. Phys.: Condens.Matter* **13** L737
- [7] Melko R G, den Hertog B C and Gingras M J P 2001 *Phys. Rev. Lett.* **87** 067203
- [8] Yoshida S, Nemoto K and Wada K 2004 *J. Phys. Soc. Jpn.* **71** 1619
- [9] Fukazawa H, Melko R G, Higashinaka R, Maeno Y and Gingras M 2002 *Phys. Rev. B* **65** 054410
- [10] Gervais F 1983 in *Infrared and Millimetre Waves* Vol. 8 edited by Button K J (Academic, New York) p. 279
- [11] Massa N E, Campa J and Rasines I 1995 *Phys. Rev. B* **52** 15920
- [12] Tajima S, Ido T, Ishibashi S, Itoh T, Eisaki H, Mizuo Y, Arima T, Takagi H and Uchida S 1991 *Phys. Rev. B* **43** 10496
- [13] Fateley W G, Dollish F R, McDevitt N T and Bentley F F 1972 *Infrared and Raman Selection Rules for Molecular and Lattice Vibrations: The Correlation Method* (Wiley-Interscience, New York)
- [14] Kamba S, Buixaderas E and Pajaczowska A 1998 *Phys. Status Solidi A* **168** 317
- [15] Bruesch P 1986 *Phonons: Theory and Experiments II* (Springer-Verlag, Berlin) Ch. 2 p. 14
- [16] Lee J S, Noh T W, Bae J S, Yang In-San, Takeda T and Kanno R 2004 *Phys. Rev. B* **69** 214428
- [17] den Hertog B C and Gingras M J P 2000 *Phys. Rev. Lett* **84** 3430
- [18] Harris M J, Bramwell S T, McMorow D F, Zeiske T and Godfrey K W 2000 *Phys. Rev. Lett* **79** 2554
- [19] Smith D Y 1985 *Handbook of Optical Constants of Solids* (Academic, New York).
- [20] Homes C C, Vogt T, Shapiro S M, Wakimoto S, Subramanian M A and Ramirez A P 2003 *Phys. Rev. B* **67** 092106
- [21] Scott J F 1997 *Phys. Rev. B* **4** 1360

Figure captions

Figure 1 The temperature dependence of the reflectance of Dy₂Ti₂O₇ single crystal in the range of 50-1000 cm⁻¹.

Figure 2 Representative experimental and fitted reflectivity spectra of Dy₂Ti₂O₇ at (a) 300 K and (b) 10 K. Solid lines represent experimental data and dot lines are the fitting results.

Figure 3 The real part of the temperature dependent optical conductivity of Dy₂Ti₂O₇ in the far-infrared region.

Figure 4 The temperature dependence of Born effective charge per oxygen atom in Dy₂Ti₂O₇. The dots represent the deduced values at various temperatures between 300 and 10 K. Inset: the temperature dependence of the static optical permittivities.

Table 1. The phonon parameters for the Lorentzian fits to the conductivity of $Dy_2Ti_2O_7$ single crystal at different temperatures. All units are in cm^{-1} .

<i>Temperature</i>		<i>F_{1u} modes</i>							
T=300 K	Ω_{TO}	–	137	226	261	374	440	545	608
	γ_{TO}	–	23	77	44	62	26	36	18
	Ω_{LO}	–	143	253	320	437	537	608	745
	γ_{LO}	–	12	31	33	26	38	19	36
T=250 K	Ω_{TO}	–	133	224	261	372	442	544	611
	γ_{TO}	–	18	65	40	60	22	31	18
	Ω_{LO}	–	142	253	320	440	537	611	742
	γ_{LO}	–	13	29	31	22	33	19	26
T=200 K	Ω_{TO}	93	135	204	259	370	444.5	543	608
	γ_{TO}	15	23	62	26	42	16	23	17
	Ω_{LO}	93.5	144	254	322	443	538	608	746
	γ_{LO}	12	12	22	29	16	24	18	20
T=150 K	Ω_{TO}	91.5	130	199	259	370	447	544	608
	γ_{TO}	18	18	45	45	35	16	23	16.5
	Ω_{LO}	92	142	254	321	445	538	608	749
	γ_{LO}	14	13	20	29	16	25	17	28
T=100 K	Ω_{TO}	88	127	198	258	370	450	546	607
	γ_{TO}	18	12	36	20	33	19	29	20
	Ω_{LO}	90	140	252	320	447.5	537	607	748
	γ_{LO}	23	12	20	30	20	35	21	45
T=50 K	Ω_{TO}	86	127	197	259	370	453	545	612
	γ_{TO}	15	10	29	18	31	19	30	20
	Ω_{LO}	89	141	252	320	450	536	612	748
	γ_{LO}	29	15	18	28	20	34	21	45
T=10 K	Ω_{TO}	85	126	197	260	370	454	545	612
	γ_{TO}	15	7	26	17	27	18	31	22
	Ω_{LO}	90	139	253	317	451	535	612	748
	γ_{LO}	27	17	18	26	20	34	23	43

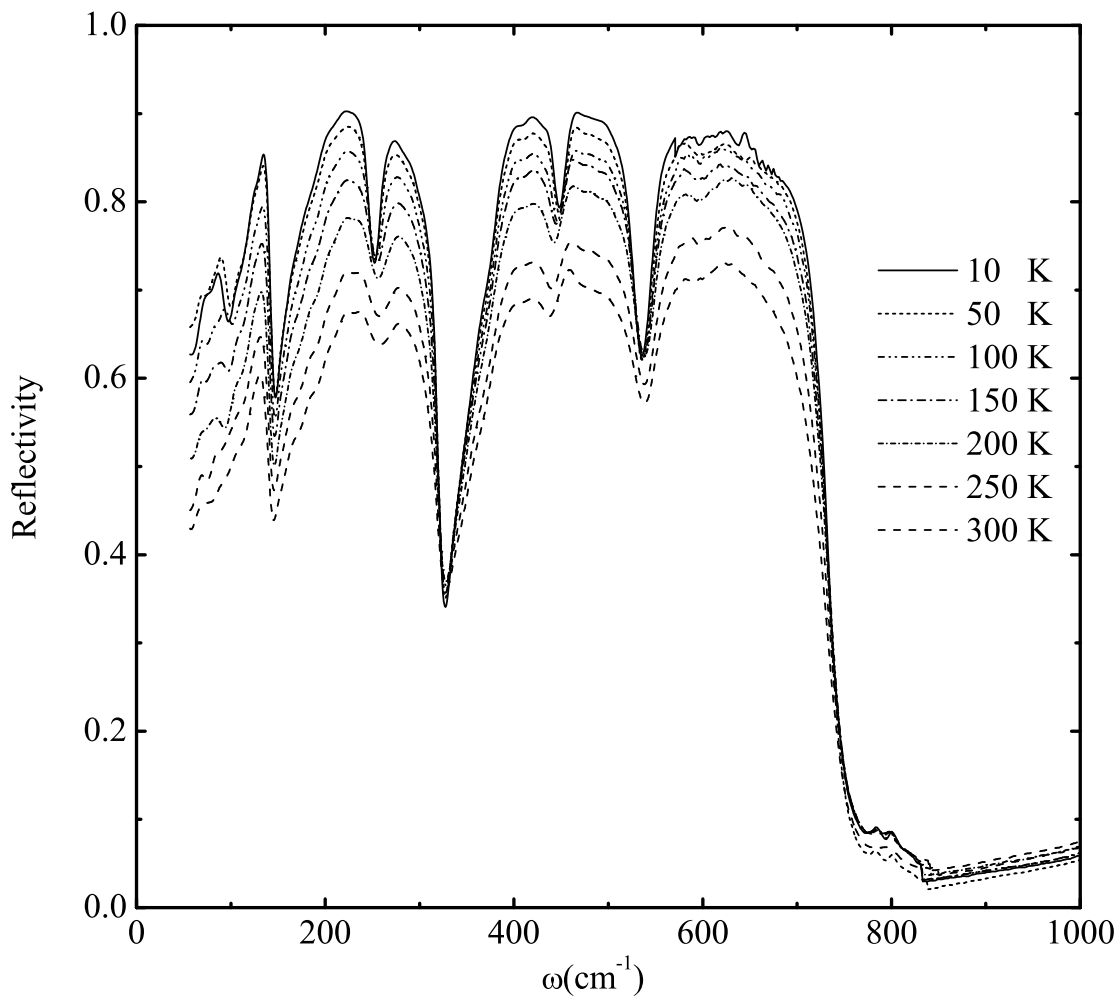


Fig.1 C.Z. Bi et al.

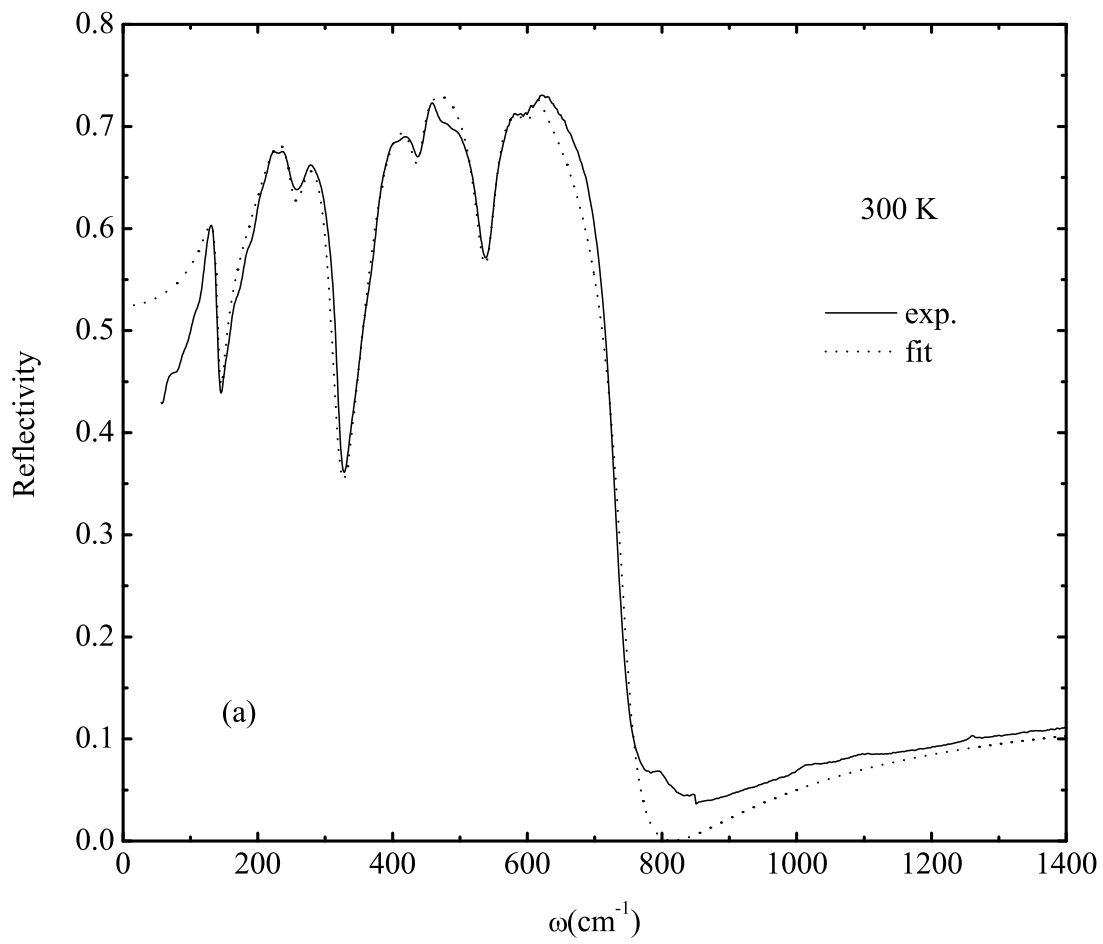


Fig.2(a) C.Z. Bi et al.

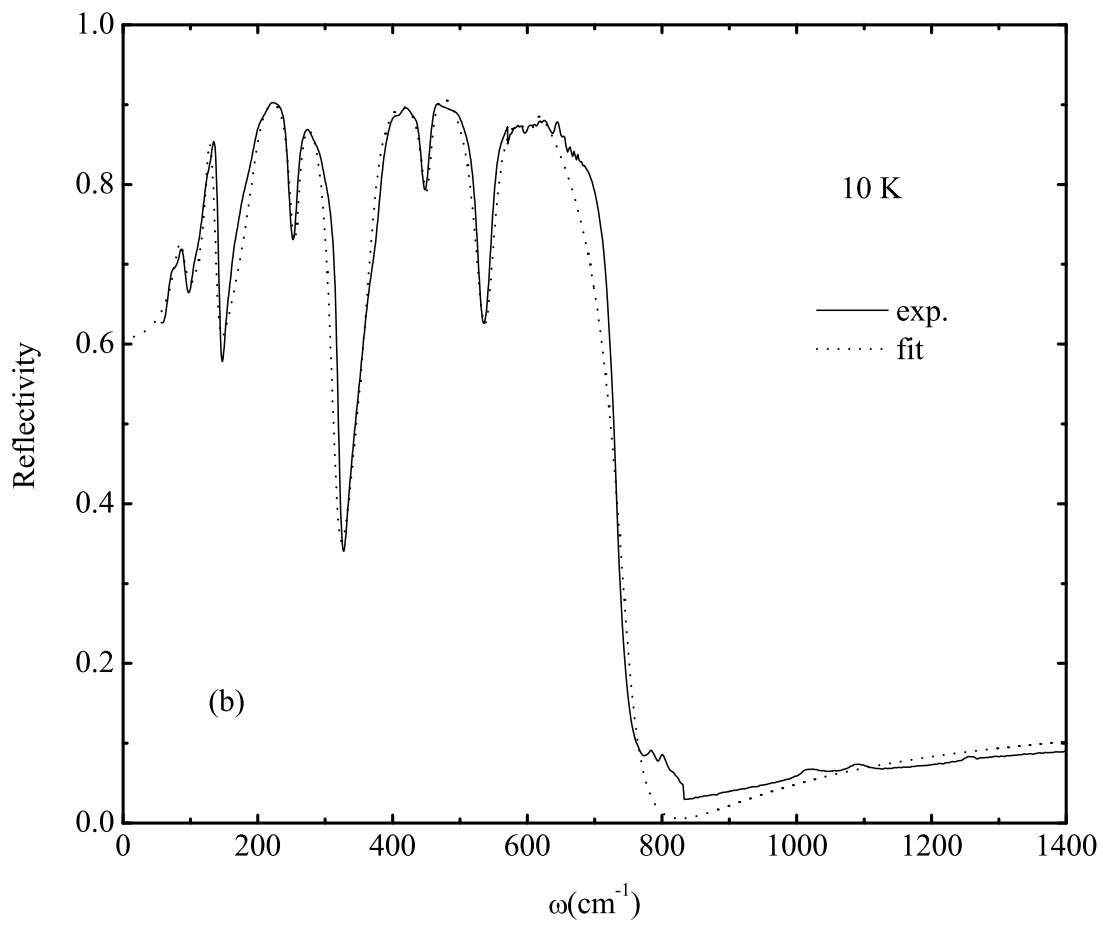


Fig.2(b) C.Z. Bi et al.

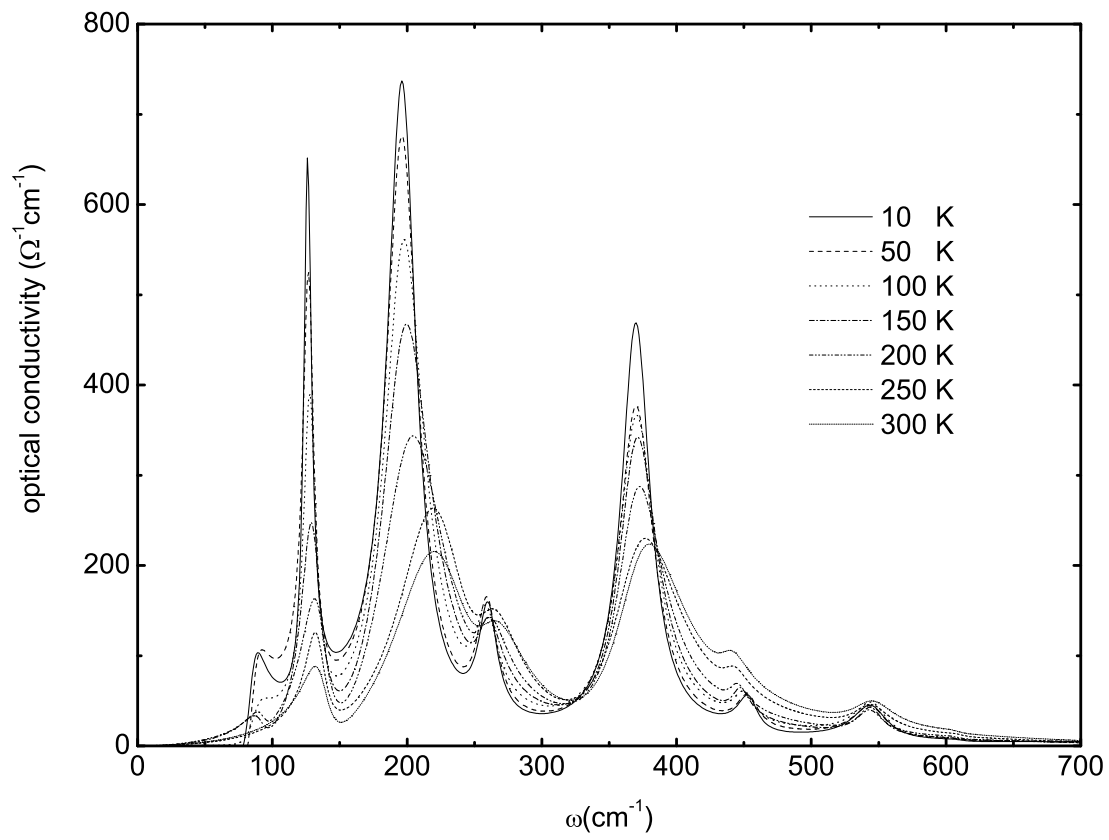


Fig.3 C.Z. Bi et al.

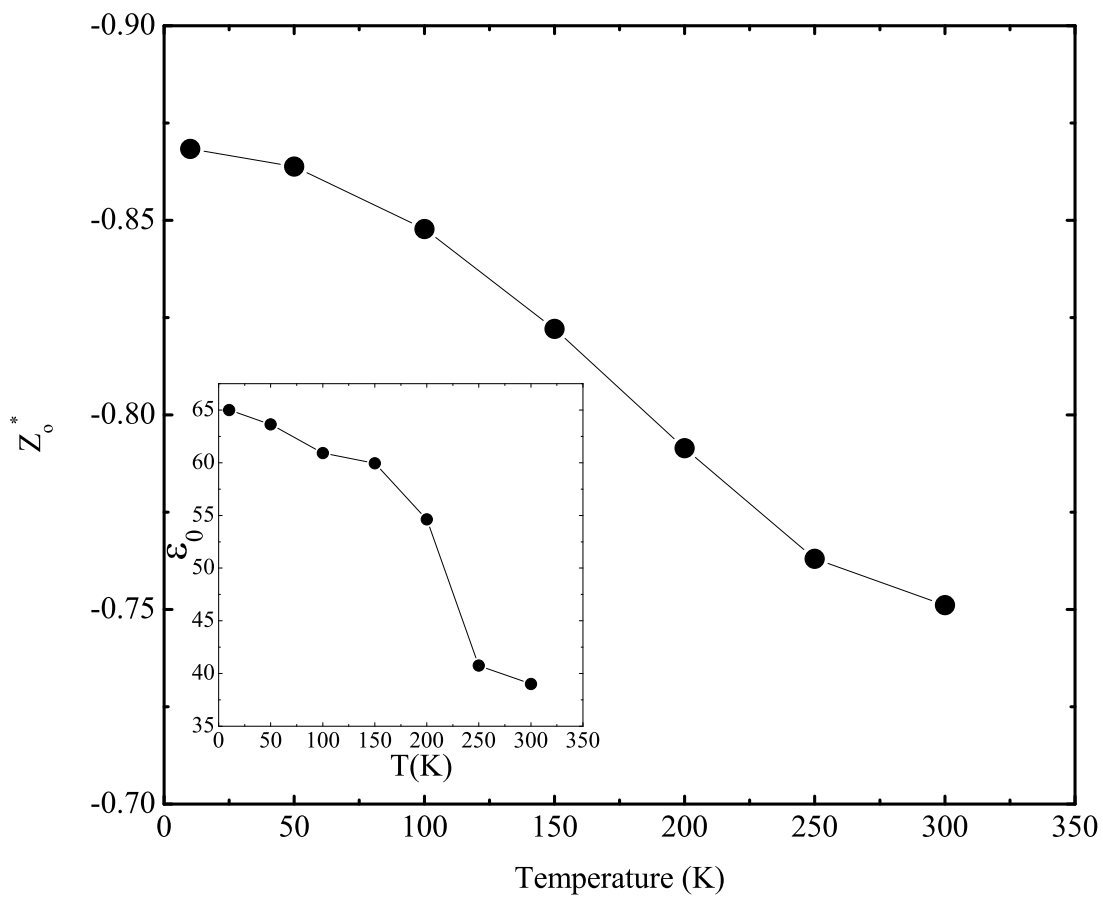


Fig.4 C.Z. Bi et al.